Journal of Pharmaceutical & Biomedical Analysis
Vol. 8, No. 2, pp. 151–158, 1990
Printed in Great Britain

0731–7085/90 $3.00 + 0.00
Pergamon Press plc

Metabolism of aromatic and heterocyclic amine bladder carcinogens: bioanalytical considerations*

MICHAEL B. MATTAMMAL,‡‖ VIJAYA M. LAKSHMI,‡‖ TERRY V. ZENSER†‡§‖ and BERNARD B. DAVIS‡‖

‡*Geriatric Research, Education and Clinical Center, Veterans Administration Medical Center, St. Louis, MO 63125, USA*
§ *Departments of Biochemistry and* ‖*Internal Medicine, St. Louis University School of Medicine, St. Louis, MO 63104, USA*

Abstract: Aromatic and heterocyclic amines are environmental chemicals which can cause bladder cancer in man. Because these chemicals cause carcinomas at a site distal to their portals of entry, metabolic processes are involved in initiation of their carcinogenic effects. *N*-[4-(5-nitro-2-furyl)-2-thiazolyl]formamide (FANFT) and its deformylated analogue, ANFT, were used as model compounds to assess metabolism. Electrochemical properties of ANFT made liquid chromatography with electrochemical detection a specific and sensitive method for analysis. Peroxidatic metabolism of ANFT by prostaglandin H synthase (PHS) in the presence of *N*-acetylcysteine resulted in the formation of 2-amino-4-(5-nitro-2-furyl)-5-(*N*-acetylcystein-*S*-yl)thiazole (ANFT–MA). This thioether product has an oxidation potential significantly lower than ANFT. Rat urinary excretion of ANFT–MA was significantly decreased with peroxidase inhibitors, 6-*n*-propyl-2-thiouracil and methimazole. Inhibitors did not alter excretion of ANFT or prostaglandin E_2, a PHS product of arachidonic acid metabolism. ^1H and ^{13}C-NMR were selected to explore potential structural differences between ANFT and FANFT which might explain preferential PHS metabolism of ANFT. Evidence for a "zwitterion" configuration for ANFT but not FANFT was observed. ANFT in the "zwitterion" configuration would be a better reducing co-substrate. Chemical synthesis and GC–MS fragmentation patterns identified 3-(2,3-dihydro-1-methyl-2-pyrrolyl)pyridine as a peroxidatic product of nicotine metabolism. This peroxidatic product was found in urine from a cigarette smoker in an amount approximately 6% that observed for cotinine. Thus, a potential rôle for peroxidative metabolism was demonstrated in man.

Keywords: *Liquid chromatography with electrochemical detection; cyclic voltammetry; chromatographically-assisted hydrodynamic voltammetry; aromatic amine-induced bladder cancer; N-[4-(5-nitro-2-furyl)-2-thiazolyl]formamide, 2-amino-4-(5-nitro-2-furyl)thiazole.*

Introduction

A majority of human cancers are thought to arise from environmental exposures as judged from epidemiological studies [1, 2]. These exposures may include diet, occupation, medications and air pollution. Bladder cancer has long been associated with occupational exposure. The classic clinical report by Rehn in 1895 detailed the occurrence of urinary bladder cancer in workers engaged in the manufacture of Fuchsin from crude aromatic amines [3]. Subsequent epidemiological studies confirmed the report of Rehn and identified 4-aminobiphenyl, 2-naphthylamine and benzidine as causative agents [4–6]. These aromatic amines cause bladder cancer in dog, the animal model for assessing aromatic amine-induced bladder cancer [7, 8]. Aromatic amines are not directly mutagenic or carcinogenic but require endogenous metabolic activation.

Aromatic amine-induced bladder tumors in the dog may take 2–5 years to appear [7, 8]. While acute metabolic studies are readily achievable in the dog, the cost and time required for long-term animal studies using the dog model make such studies difficult to accomplish. Rodents fed aromatic amines develop a very high incidence of liver, not bladder, cancer. This has been attributed to the rapid acetylation of the amines and subsequent oxidation by hepatic mixed-function oxidases [9].

A rat model has been developed using *N*-[4-(5-nitro-2-furyl)-2-thiazolyl]formamide (FANFT) (Fig. 1) [10]. Rats fed FANFT at 0.2% of the diet for 10 or more weeks develop a high incidence (80–100%) of bladder cancer.

*Presented at a Symposium at the 40th Pittsburgh Conference and Exposition, Atlanta, Georgia, March 1989.

† Address correspondence to: Dr Terry V. Zenser, GRECC (111G-JB), VA Medical Center, St. Louis, MO 63125, USA.

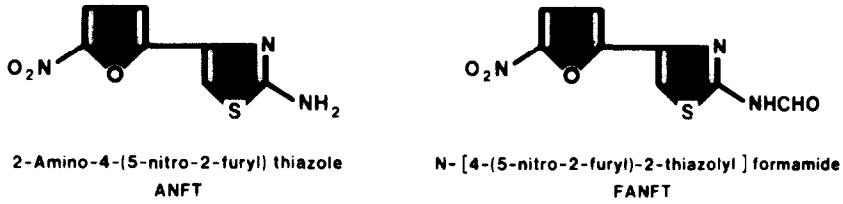

Figure 1
Structures, chemical names, and abbreviations of the 2-aminothiazoles used to study bladder cancer in the rat.

The lesions are irreversible and eventually result in bladder carcinomas within 1 year. A two-stage model for FANFT-induced bladder cancer has also been developed. Histologic characteristics of FANFT-induced tumors are similar to those reported for humans. ANFT, deformylated FANFT, is thought to be the proximate carcinogen in FANFT-induced bladder cancer. This is because the mutagenicity of urine from FANFT-fed animals and the susceptibility of different species to FANFT-induced urothelial cancer correlate with urinary levels of ANFT rather than FANFT. Paradoxically, dietary FANFT is more carcinogenic than dietary ANFT. This phenomenon has been attributed to renal metabolic/excretory coupling in which FANFT excretion is coupled to renal deformylation [11].

Work in this laboratory has been directed at understanding the metabolic processes involved in initiating aromatic amine-induced bladder cancer [12, 13]. Initiation results in the fixation of a chemical mutation(s) which, following promotion, has the potential to cause tumor formation. Initiation by chemicals is thought to result in the formation of DNA adducts which cause the heritable changes characteristic of carcinogenesis [14, 15]. Because the FANFT rat model affords the opportunity for *in vivo* testing of hypotheses, the initiation of FANFT/ANFT-induced bladder cancer has been studied. This review will concentrate on the bioanalytical aspects of these studies.

Analytical Considerations

Metabolic and physiological parameters affecting absorption, metabolism and disposition of FANFT/ANFT have been major areas of investigation. The major bioanalytical problems associated with this project have been quantitation and identification of these carcinogens and their unknown metabolites. Quantitation is a particularly difficult aspect because radiolabelled FANFT/ANFT is not commercially available. A synthetic procedure for making ^{14}C-FANFT/ANFT was developed. However, the high cost and low specific activity of ^{14}C-thiourea used in the synthesis did not make this an attractive proposition. For this reason, the electrochemical properties of ANFT, the more proximate carcinogen, have been particularly useful in assessing oxidative metabolism.

Cyclic voltammetry was used to measure the oxidation and reduction potential of ANFT [16]. The voltammogram (Fig. 2) indicates the half-wave potentials for ANFT oxidation and reduction of approximately +700 and −500 mV, respectively. These potentials are indicative, respectively, of the 2-aminothiazole and 5-nitrofuran rings. Thus, monitoring high-performance liquid chromatography (HPLC) eluents at +700 and −500 mV allows for quantitation and provides information about the electrochemical properties of ANFT metabolites.

Peroxidatic Metabolism by Prostaglandin H Synthase

Peroxidatic metabolism of ANFT by prostaglandin H synthase (PHS) has been proposed as one mechanism for metabolism [12, 13]. PHS is a haemprotein consisting of two separate enzymatic activities: a fatty acid cyclooxygenase and a prostaglandin hydroperoxidase [17]. The former utilizes specific polyunsaturated fatty acids as substrates, i.e. arachidonic acid, and is inhibited by non-steroidal anti-inflammatory drugs, i.e. aspirin and indomethacin. In contrast, the hydroperoxidase activity does not have specific substrates or inhibitors and is not inhibited by non-steroidal anti-inflammatory drugs. Prostaglandin (PG) H_2, the product of arachidonic acid metabolism by PHS, is converted to a variety of prostaglandins and thromboxane.

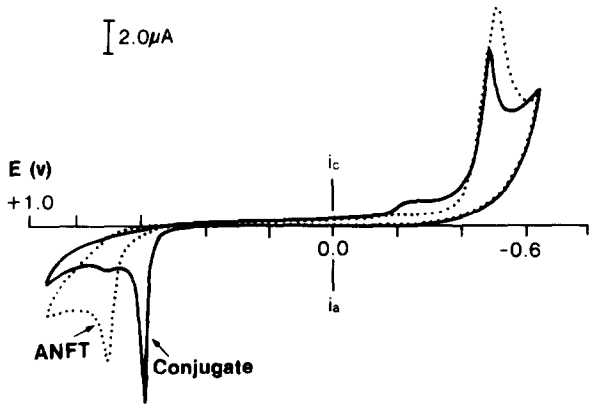

Figure 2
Illustration of the cyclic voltammetric method used to measure oxidation and reduction potentials. Voltammograms of ANFT and ANFT–MA (each at 0.1 mM) were obtained in ethanol–0.1 M sodium phosphate, pH 7.0 (1:9). Data were recorded with a stationary carbon paste electrode at a scan rate of 200 mV s^{-1}. The scan was initiated in the positive direction of 0.0 V versus Ag/AgCl.

These biologically important compounds derived from fatty acids are well-known for their effects on cellular and organ function [18, 19]. The hydroperoxidase activity of PHS requires a reducing co-substrate. The natural reducing co-substrate(s) is not known. However, certain aromatic and heterocyclic amines can function as reducing co-substrates. Following oxidation, some amines become activated and bind nucleophiles such as glutathione and DNA [12, 13].

Incubation of ANFT with PHS in the presence of arachidonic acid and glutathione resulted in the formation of a new product (conjugate) [20]. Conjugate formation was demonstrated (peak A) by HPLC with electrochemical detection (Fig. 3, panel 1). The formation of this product was prevented if indomethacin, an inhibitor of PHS, was present (Fig. 3, panel 2). Therefore, PHS can activate ANFT to bind nucleophiles.

Using a dual-electrode electrochemical detector, simultaneous monitoring at +800 and −550 mV demonstrated that the conjugate had intact aminothiazole and nitrofuran rings. Substitution of cysteine or *N*-acetylcysteine for glutathione resulted in changes in the HPLC elution profile consistent with formation of the respective thioether conjugate of ANFT. Absorption spectra obtained with a photodiode array detector demonstrated that eluents had maxima at 275–300 and 380–410 nm. These maxima are also consistent with intact aminothiazole and nitrofuran rings. The formation of thioether conjugates of ANFT provided a means for assessing ANFT per-

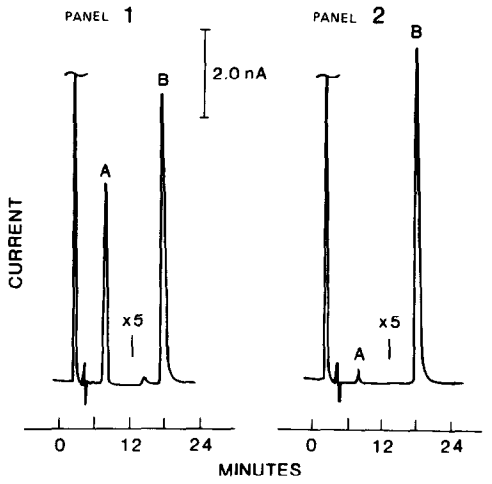

Figure 3
Metabolism of ANFT by PHS. Incubation mixtures contained solubilized ram seminal vesicle microsomal PHS (0.1 μg ml^{-1}), 0.05 mM ANFT, 1.0 mM glutathione, and 100 mM phosphate buffer, pH 7.0. Reactions were initiated by addition of 0.1 mM arachidonic acid. The HPLC mobile phase consisted of methanol–0.1 mM ammonium acetate, pH 6.0 (35:65) at a flow rate of 1 ml min^{-2}. ANFT (peak B) and its glutathione conjugate (peak A) were quantitated amperometrically at +750 mV versus Ag/AgCl. Panels 1 and 2 are in the absence and presence of 0.1 mM indomethacin, respectively [23].

oxidatic metabolism *in vivo*. For this reason, identification of the suspected conjugate was undertaken.

Comparison of Synthetic to Authentic (Enzymatic) Conjugate

A method for chemical synthesis of conjugate was developed because only small amounts of conjugate could be obtained by

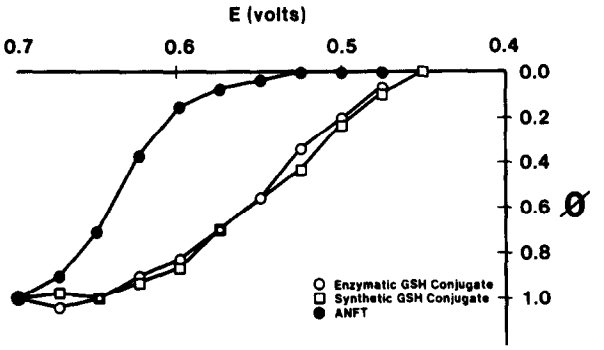

Figure 4
Comparison of enzymatic and synthetic glutathione conjugates of ANFT using chromatographically-assisted hydrodynamic voltammograms. See text for details. HPLC was conducted as described in Fig. 3 [20].

enzymatic synthesis [20]. It was important to know whether the synthetic conjugate was identical to the PHS-derived conjugate. Chromatographically-assisted hydrodynamic voltammetry was one technique used for this purpose. Figure 4 illustrates a plot of this data. Samples of synthetic or enzymatic derived conjugate were repetitively chromatographed and the applied detector potential altered as indicated. The peak heights were normalized and expressed as a fraction of the value obtained at the largest potential utilized ($\phi = 1$). As shown in Fig. 4, plots of enzymatic and synthetic glutathione conjugate were identical. Thus, identical chromatographic, electrochemical and other properties demonstrated the synthetic conjugate to be the same as the enzymatic conjugate.

The thioether conjugate was considerably easier to oxidize than ANFT itself. As indicated in Fig. 4, the peak potential for oxidation of ANFT is approximately 100 mV higher than its conjugate. The voltammogram in Fig. 2 also illustrates this phenomenon. However, note that the conjugate exhibits a reduction peak very similar to ANFT. This suggests that the aminothiazole moiety rather than the 5-nitrofuran ring has been altered by oxidation and subsequent conjugation.

The *N*-acetylcysteine conjugate of ANFT (ANFT–MA) was anticipated as a urinary metabolite from rats fed FANFT/ANFT. Therefore, synthetic ANFT–MA was compared to enzymatically derived conjugate using parallel dual-electrode detection. Enzymatic and synthetic derived samples were injected separately and as a 50:50 mixture of each solution. For each sample, the ratio of peak heights obtained at applied potentials of +750 and +550 mV was recorded. Two different chromatographic systems were used. Systems were optimized such that the capacity factor k' of the product (a generalized expression of retention) differed by a factor of 10. Ratios observed with enzymatic and synthetic samples were not different from one another or from that observed with the mixture. Chromatographic retention times were also not different. Thus, synthetic and enzymatic derived conjugate were identical.

Identification of Peroxidatic Product

Synthetic *N*-acetylcysteine conjugate was used for structural characterization by ^{1}H and ^{13}C-NMR [20]. Assignments of protons and carbon atoms in the conjugate were made by comparison with spectra obtained with ANFT and *N*-acetylcysteine under identical conditions. Proton spectra of ANFT and ANFT–MA were identical except for the absence of the C-5 proton in ANFT–MA (Fig. 5). Chemical shifts of the major carbon atoms in these compounds were very similar. However, in the conjugate, C-5 of thiazole is shifted significantly downfield without splitting indicating the lack of a proton. Based on electrochemical, UV–vis. and magnetic resonance spectral data, it was concluded that ANFT–MA is substituted in the C-5 position of the aminothiazole ring with the sulphur atom of *N*-acetylcysteine. This structure was subsequently confirmed by high resolution mass spectrometry. The lower oxidation potential of ANFT–MA relative to ANFT would appear to be the result of electron-donating inductive effects by the lone electron pair of the exocyclic sulphur atom increasing the electron density of the thiazole. Ring-substituted thioether conjugates of acetaminophen [21] and hydroquinone [22]

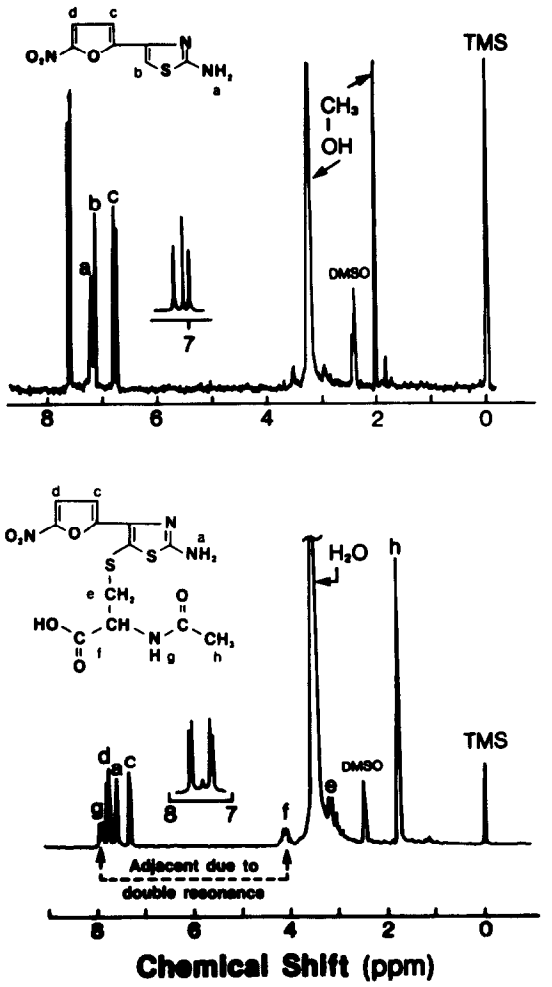

Figure 5
^1H NMR spectra of ANFT (top) and ANFT–MA (bottom). Compounds were dissolved in d_6-DMSO and spectra obtained with Jeol FX-100 100 MHz spectrometer. Inserts demonstrate absence of amine peaks after D_2O addition due to D:H exchange [20].

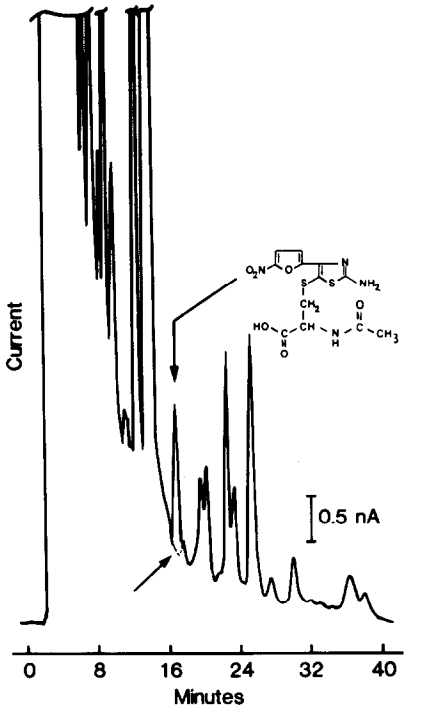

Figure 6
HPLC chromatograph of an 18-h urine sample (0.02 ml) obtained from rats treated p.o. with 150 mg/kg FANFT. The elution of ANFT–MA in urine from treated rats is illustrated along with its absence in urine from untreated rats (lower arrow, dashed line). HPLC was conducted as described in Fig. 3 [23].

have also been reported to exhibit a decreased oxidation potential.

In Vivo Identification of Peroxidatic Product

A whole animal study was designed to assess the presence of ANFT–MA in urine from rats fed FANFT [23]. In separate treatment groups, the peroxidase inhibitors, 6-*n*-propyl-2-thiouracil and methimazole, were orally administered to rats 30 min before FANFT. Urine was collected for 18 h and analysed for ANFT, ANFT–MA and PGE_2. As indicated in Fig. 6, ANFT–MA was observed in FANFT-treated but not control rats. The authenticity of the urinary ANFT–MA was verified by chromatographically-assisted hydrodynamic voltammetry as described above. Urinary ANFT–MA was shown to be identical to synthetic ANFT–MA by this procedure. Actual amounts of ANFT–MA recovered in urine are tabulated in Table 1. The amount of ANFT–MA present in urine (14.8 ± 2.1 nmol/18 h) was approximately 5% that observed for ANFT (307 ± 47 nmol/18 h). Administration of either 6-*n*-propyl-2-thiouracil or methimazole significantly reduced the excretion of ANFT–MA but did not alter ANFT. PGE_2, an indicator of urinary tract PHS activity, was determined by radioimmunoassay. Excretion of PGE_2 was not altered by any of these treatments.

This experiment provides the first demonstration of an oxidative product of ANFT metabolism *in vivo*. The reduction of ANFT–MA but not ANFT excretion by peroxidase inhibitors suggests decreased peroxidatic metabolism of ANFT–MA. As peroxidases are ubiquitously distributed in mammalian tissues [12], a variety of peroxidases, in addition to PHS, may be involved in ANFT metabolism. However, previous experiments have demonstrated a lack of metabolism of ANFT by

Table 1
Effect of propylthiouracil and methimazole on urinary metabolites from rats dosed with FANFT*

Condition	PGE_2 (ng/18 h)†	ANFT (nmol/18 h)†	ANFT–MA (nmol/18 h)†
Control (5)‡	174 ± 34	307 ± 47	14.8 ± 2.1
+250 mg/kg PTU (5)	178 ± 28	293 ± 82	7.9 ± 0.8§
+167.5 mg/kg MMI (4)	150 ± 43	278 ± 43	6.2 ± 1.1§

*Rats were pretreated p.o. with dimethyl sulphoxide or inhibitor 30 min prior to p.o. dosing with 150 mg/kg FANFT [23].
†Mean ± SE of amounts excreted in 18 h postdose.
‡Numbers in parentheses, number of rats per group.
§Significantly different from control at $P < 0.02$.

several peroxidases [24]. Decreasing ANFT–MA excretion by processes other than inhibition of peroxidase metabolism seems unlikely since both 6-*n*-propyl-2-thiouracil and methimazole would have to exert the same inhibition on the same non-peroxidatic process. The lack of effect of these inhibitors on PGE_2 excretion is consistent with their effect on the hydroperoxidase rather than cyclooxygenase activity of PHS. These results are also consistent with whole animal feeding studies in which aspirin, an inhibitor of arachidonic acid initiated ANFT metabolism by PHS, has been shown to reduce the early morphological lesions and incidence of FANFT-induced bladder cancer [25–27].

The success of the *in vivo* metabolic study depended to a great extent on combining the selectivity of liquid chromatography with the specificity and high sensitivity of electrochemical detection. This technique allowed the determination of 5–10 pmol of ANFT–MA in urine without prior purification. Urine samples (0.02 ml) were injected directly on the HPLC. Since the experiment was designed to mimic FANFT feeding studies, animals were orally dosed with 150 mg/kg FANFT. This is the calculated daily amount of dietary FANFT received during feeding studies [25–27]. The high dose of FANFT administered precluded using entirely radiolabelled FANFT in these experiments. In addition, even inclusion of modest amounts of radioactivity was considered theoretically unfeasible because the amount of ANFT–MA in urine was anticipated to be considerably less than ANFT, which was known to be about 5% of the administered dose of FANFT. This assumption was found to be correct with ANFT–MA representing approximately 0.25% of the original dose of FANFT administered. Thus, the development of the methodology for quantitating and identifying ANFT–MA by liquid chromatography with electrochemical detection proved invaluable for the *in vivo* studies.

Possible Mechanism of Peroxidatic Metabolism

The mechanism by which ANFT is activated by PHS was investigated. Previous studies had demonstrated a preferential PHS metabolism of ANFT compared to FANFT [28]. ^{1}H and ^{13}C-NMR were selected to explore potential structural differences between ANFT and FANFT which might explain preferential PHS metabolism [29]. A proton transfer from the C-5 of ANFT was observed. As shown in Fig. 7, the doublet due to the H-5′ proton of ANFT (Fig. 7a) decreased after 1 week (Fig. 7b) and was significantly decreased after 4 months (Fig. 7c). A corresponding new ^{13}C signal was observed at 169.25 ppm (not shown). These results were interpreted to indicate that the proton at C-5 migrated to the endocyclic nitrogen at N-3. This "zwitterion" configuration is illustrated in Scheme 1. FANFT showed no evidence of a "zwitterion" formation by either ^{1}H or ^{13}C-NMR. FANFT showed a different proton-transfer reaction which involved the amide proton. ^{15}N chemical shifts, line widths and heteronuclear ^{1}H–^{15}N and ^{15}N–^{15}N coupling constants also support Scheme 1.

The "zwitterion" configuration observed with ANFT is envisioned as a structure which could be facilitated by the catalytic properties of PHS. ANFT in the "zwitterion" configuration would be a better reducing co-substrate. Thus, differences in the chemistry of the thiazole ring caused by formylation may partially explain the differential peroxidatic activation of ANFT compared with FANFT.

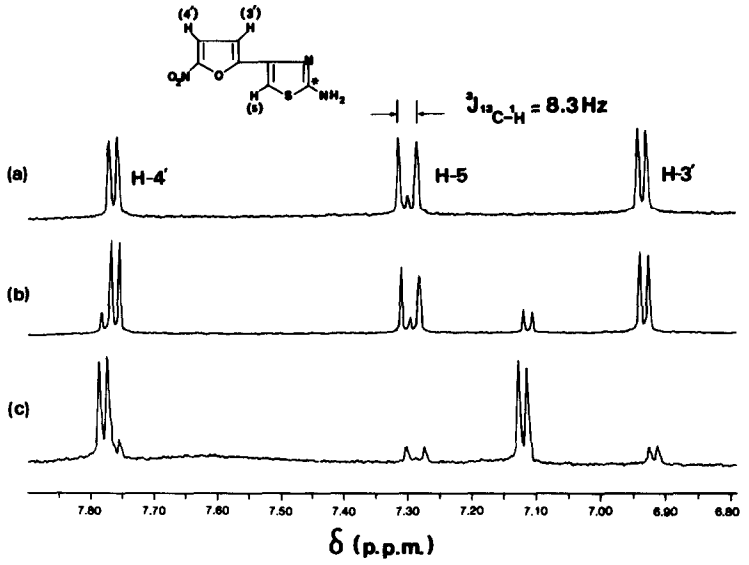

Figure 7
(a) The ^1H spectrum of 19 mM ANFT-[2-^{13}C] in DMSO-d_6 at 20.6°C immediately after dissolving the sample (pre-equilibrium spectrum), showing the heteronuclear ^1H–^{13}C coupling constant. (b) The same sample after *ca* 1 week at room temperature revealing the additional presence of the presumed "zwitterion" of ANFT. (c) The same sample after *ca* 4 months at room temperature revealing the presumed final equilibrium ratio of the ANFT and ANFT "zwitterion". Spectra were obtained at 300 MHz on a Varian XL-300 spectrometer [29].

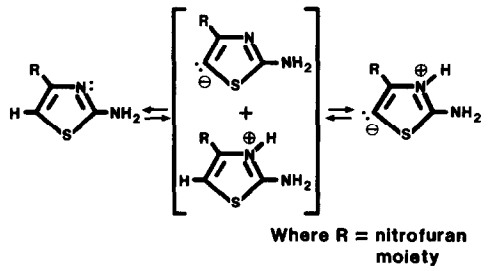

Scheme 1

Correlative Studies in Man

While the FANFT/ANFT rat model provided a means of testing hypotheses in animals, this information does not directly relate to bladder cancer in man. However, two areas of our research endeavor have supported a rôle for peroxidatic metabolism in bladder cancer in man. The first area involves investigation of the arachidonic acid cascade in cultured human urothelial cells [30, 31]. These studies measured hormonal mediated release of prostaglandins demonstrating the presence of PHS in urothelial cells and thus, the capability for peroxidatic activation of aromatic amine bladder carcinogens. The second area involved the study of nicotine metabolism [32]. Using lung microsomes prepared from rabbit, both mixed-function oxidase and PHS metabolism of nicotine were demonstrated. Cotinine was the major mixed-function oxidase product. PHS formed a previously unidentified metabolite. GC–MS fragmentation patterns contributed to the identification of this metabolite but could not locate the exact position of the double bond in the pyrrolyl ring (Fig. 8). Chemical synthesis provided this additional information. Reduction of cotinine yielded the new metabolite demonstrating that it is a delta-4,5-enamine. 3-(2,3-Dihydro-1-methyl-2-pyrrolyl)pyridine was found in urine from a cigarette smoker in an amount approximately 6% that observed for cotinine. Thus, peroxidatic metabolism of nicotine was demonstrated in man, suggesting a potential rôle for peroxidative metabolism of other xenobiotics.

Conclusions

A combination of bioanalytical and synthetic techniques are providing important new information about the metabolic processes involved in initiating aromatic amine-induced bladder cancer. Investigation of FANFT/ANFT metabolism has relied heavily on liquid chromatography with electrochemical detection. Metabolism of the aromatic amine bladder carcinogen, benzidine, has also been studied in a similar manner [33]. Liquid chromatography

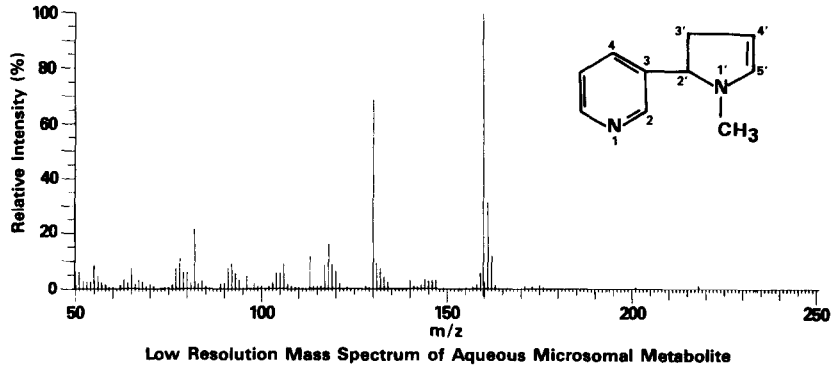

Figure 8
Low resolution mass spectrum of aqueous PHS product of nicotine metabolism, 3-(2,3-dihydro-1-methyl-2-pyrrolyl) pyridine. Spectra were obtained with a Finnigan model 3290 GC–MS [32].

with electrochemical detection is amenable to studies using other aromatic amine carcinogens and perhaps one will see more use for this technique in future studies.

Acknowledgements — This work was supported by grants from the Veterans Administration, CA-28015 from the National Cancer Institute and BC-700 from the American Cancer Society. The authors acknowledge the efforts of Drs John R. Rice and Robert M. Davidson for their contributions to electrochemical and NMR measurements, respectively. The authors appreciate the expert assistance of Sandy Melliere in preparation of the manuscript.

References

[1] J. Higginson, *Can. Cancer Conf.* **8**, 40–75 (1969).
[2] R. Doll and R. Peto, *J. Natn. Cancer Inst.* **66**, 1192–1308 (1981).
[3] L. Rehn, *Arch. Klin. Chir.* **50**, 588–600 (1895).
[4] R.A.M. Case, M.W. Hosker, D.B. McDonald and J.T. Pearson, *Br. J. Ind. Med.* **11**, 75–104 (1954).
[5] W.F. Melick, H.M. Escue, J.J. Naryka, R.A. Mezera and E.R. Wheeler, *J. Urol.* **74**, 760–766 (1955).
[6] T.F. Mancuso and A.A. El-Attar, *J. Occup. Med.* **9**, 277–285 (1967).
[7] J.L. Radomski, *A. Rev. Pharmac. Toxicol.* **19**, 129–157 (1979).
[8] T.J. Haley, *Clin. Toxicol.* **8**, 13–42 (1975).
[9] C.N. Martin, F.A. Beland, R.W. Roth and F.F. Kadlubar, *Cancer Res.* **42**, 2678–2686 (1982).
[10] S.M. Cohen, in *Carcinogenesis: A Comprehensive Survey* (G.T. Bryan, Ed.), pp. 171–231. Raven Press, New York (1978).
[11] L.A. Spry, J. Rubinstein, C. Rettke, T.V. Zenser and B.B. Davis, *Am. J. Physiol.* **254F**, 145–152 (1988).
[12] T.V. Zenser and B.B. Davis, in *Biochemistry of Arachidonic Acid Metabolism* (W.E.M. Lands, Ed.), pp. 127–149. Martinus Nijhoff, Boston (1985).
[13] T.V. Zenser and B.B. Davis, *Prostaglandins, Leukotrienes and Essential Fatty Acids: Rev.* **31**, 199–207 (1988).
[14] E. Farber, *Cancer Res.* **44**, 4217–4223 (1984).
[15] I.B. Weinstein, *Cancer Res.* **48**, 4135–4143 (1988).
[16] J.R. Rice, T.V. Zenser and B.B. Davis, in *Arachidonic Acid Metabolism and Tumor Initiation* (L.J. Marnett, Ed.), pp. 125–169. Martinus Nijhoff, Boston (1985).
[17] S. Ohki, N. Ogino, S. Yamamoto and O. Hayaishi, *J. Biol. Chem.* **254**, 829–836 (1979).
[18] W.E.M. Lands, *A. Rev. Physiol.* **41**, 633–652 (1979).
[19] B. Samuelsson, S.-E. Dahlen, J.A. Lindgren, C.A. Rouzer and C.N. Serhan, *Science* **237**, 1171–1176 (1987).
[20] J.R. Rice, T.V. Zenser and B.B. Davis, *Carcinogenesis (Lond.)* **6**, 585–590 (1985).
[21] D.J. Miner, J.R. Rice, R.M. Riggin and P.T. Kissinger, *Analyt. Chem.* **53**, 2258–2263 (1981).
[22] S.M. Lunte and P.T. Kissinger, *Chem. Biol. Interact.* **47**, 195–212 (1983).
[23] J.R. Rice, L.A. Spry, T.V. Zenser and B.B. Davis, *Cancer Res.* **48**, 304–309 (1988).
[24] R.W. Wise, T.V. Zenser and B.B. Davis, *Cancer Res.* **43**, 1518–1522 (1983).
[25] S.M. Cohen, T.V. Zenser, G. Murasaki, S. Fukushima, M.B. Mattammal, N.S. Rapp and B.B. Davis, *Cancer Res.* **41**, 3355–3359 (1981).
[26] G. Murasaki, T.V. Zenser, B.B. Davis and S.M. Cohen, *Carcinogenesis (Lond.)* **5**, 53–55 (1984).
[27] T. Sakata, R. Hasegawa, S.L. Johansson, T.V. Zenser and S.M. Cohen, *Cancer Res.* **46**, 3903–3906 (1986).
[28] T.V. Zenser, M.O. Palmier, M.B. Mattammal, R.I. Bolla and B.B. Davis, *J. Pharmac. Exp. Ther.* **227**, 139–143 (1983).
[29] R.M. Davidson, J.R. Rice, V.M. Lakshmi, T.V. Zenser and B.B. Davis, *Magn. Reson. Chem.* **26**, 482–487 (1988).
[30] A. Danon, T.V. Zenser, D.L. Thomasson and B.B. Davis, *Cancer Res.* **46**, 5676–5681 (1986).
[31] T.V. Zenser, D.L. Thomasson and B.B. Davis, *Carcinogenesis* **9**, 1173–1177 (1988).
[32] M.B. Mattammal, V.M. Lakshmi, T.V. Zenser and B.B. Davis, *J. Pharmac. Exp. Ther.* **242**, 827–832 (1987).
[33] R.W. Wise, T.V. Zenser, J.R. Rice and B.B. Davis, *Carcinogenesis* **7**, 111–115 (1986).

[*Received for review 7 March 1989*]